Dalton Transactions

PAPER

View Article Online
View Journal | View Issue

Cite this: *Dalton Trans.*, 2019, **48**, 11565

Mono- and bimetallic pentacoordinate silicon complexes of a chelating bis(catecholimine) ligand†

Thomas H. Do and Seth N. Brown *

Received 11th June 2019,
Accepted 4th July 2019

DOI: 10.1039/c9dt02475a

rsc.li/dalton

Schiff base condensation of 4,5-diamino-9,9-dimethylxanthene with 4,6-di-*tert*-butylcatechol-3-carboxaldehyde affords the bis(catecholimine) ligand $XbicH_4$, which can bind metals in both a square bis(catecholate) upper pocket and a pentagonal N_2O_3 lower pocket. Metalation with $PhSiCl_3$ results in $[(XbicH_2)SiPh][HCl_2]$, where the silicon adopts a five-coordinate, square pyramidal geometry in the upper pocket and the lower pocket binds to two protons on the imine nitrogens. Deprotonation of the imines with LiO^tBu, $NaN[SiMe_3]_2$, or AgOAc results in binding of the univalent metal ion in the lower pocket, where it adopts an unusual pentagonal monopyramidal geometry in the solid state. The complexes show irreversible electrochemistry, with oxidations taking place at relatively high potentials.

Introduction

Catecholate ligands are prototypical examples of redox-active ligands, and numerous complexes of fully reduced, dianionic catecholates, as well as singly oxidized, radical anion semiquinones, are known.[1] In contrast, while appropriately substituted free organic 1,2-benzoquinones are stable, metal complexes of these compounds are scarce,[2,3] presumably due to their low Lewis basicity. Metal benzoquinone complexes appear to be generated when catecholates of redox-inert metals are oxidized by oxygen atom donors, a process dubbed "nonclassical oxygen atom transfer".[4,5] However, free benzoquinone dissociates rapidly from these complexes, vitiating their ability to act as catalysts in oxygen atom transfer reactions.

One strategy to enhance binding of benzoquinones is to use polycatecholate ligands in order to tap the chelate effect to inhibit dissociation of the oxidized forms of the ligands. Isoelectronic 2-amidophenoxide ligands have been linked to form chelating bis-[6–11] or tris-amidophenoxide[12] ligands, and this strategy has been used in oxidative catalysis.[6,13–15] In all these ligands, the amidophenoxides are linked by the nitrogen substituent, an architecture that is unavailable to catecholates. Inspired by the tris-catecholate siderophore enterobactin,[16] a number of synthetic tris-catechol ligands have been prepared, where the linkers have been attached through amide or imine linkages *ortho* to the catechol group.[17] In contrast to the numerous tris(catechols), bis(catechol) ligands, which would be more attractive as ancillary ligands for catalysis, are scarce. Furthermore, the ligands that have been explored have been derived from simple 2,3-dihydroxybenzoic acid or -benzaldehyde, without further substituents *ortho* to the catechol that might be useful in stabilizing their semiquinone or quinone forms.

Recently, Arsenyev and coworkers reported the preparation of an electron-rich and sterically encumbered catecholaldehyde, 4,6-di-*tert*-butyl-2,3-dihydroxybenzaldehyde,[18] including a large-scale procedure that produces the compound in a single step by Duff reaction of commercially available 3,5-di-*tert*-butylcatechol.[19] This aldehyde readily forms imines[20] and azines, and the azines have been used to form catecholate complexes with main group elements.[21,22] Diiminobiscatecholates have been prepared, but their geometry has been such as to allow only bimetallic complexes, not chelation of two catecholates to a single metal center.[23]

Here we describe the preparation of a bis(iminocatechol) ligand that is geometrically disposed to form bis(catecholate) complexes of a single metal center, with the four oxygen atoms forming a roughly square array around the metal. Binding a metal in this pocket creates a second, crown-like, N_2O_3 donor set, which can bind to either protons, or to univalent ions such as lithium, sodium, or silver.

Department of Chemistry and Biochemistry, University of Notre Dame, 251 Nieuwland Science Hall, Notre Dame, IN 46556-5670, USA.
E-mail: Seth.N.Brown.114@nd.edu

† Electronic supplementary information (ESI) available: Additional thermal ellipsoid plot, spectra, cyclic voltammograms and computational data. CCDC 1922351–1922355. For ESI and crystallographic data in CIF or other electronic format see DOI: 10.1039/c9dt02475a

Experimental

General procedures

Unless otherwise noted, syntheses were carried out in a nitrogen-filled drybox. When dry solvents were needed, they were

purchased from Acros Organics and stored in the glovebox. 4,5-Diamino-9,9-dimethylxanthene[24] and 4,6-di-*tert*-butyl-2,3-dihydroxybenzaldehyde[19] were prepared according to literature procedures. All other reagents were commercially available and used without further purification. Except as noted, NMR spectra were acquired in CD_2Cl_2 (Cambridge Isotope Laboratories), which was dried over 4 Å molecular sieves, followed by CaH_2, and stored in the drybox prior to use. NMR spectra were measured on a Bruker Avance DPX 400 MHz or 500 MHz spectrometer. Chemical shifts are reported in ppm downfield of TMS, with ^{1}H and $^{13}C\{^1H\}$ spectra referenced using the known chemical shifts of the solvent residuals and $^{29}Si\{^1H\}$ spectra referenced to TMS as an internal standard. Infrared spectra were recorded by ATR on a Jasco 6300 FT-IR spectrometer and are reported in wavenumbers. UV-visible spectra were recorded in 1 cm quartz cells on a ThermoFisher Evolution Array diode array spectrophotometer. Elemental analyses were performed by M-H-W Laboratories (Phoenix, AZ, USA).

Syntheses

9,9-Dimethylxanthene-4,5-bis(4,6-di-*tert*-butyl-2,3-dihydroxybenzaldimine) ($XbicH_4$). In a 50 mL round-bottom flask in the air, 4,5-diamino-9,9-dimethylxanthene (0.387 g, 1.61 mmol) and 4,6-di-*tert*-butyl-2,3-dihydroxybenzaldehyde (0.886 g, 3.54 mmol) are dissolved in 20 mL of methanol. The reaction mixture is refluxed for 17 hours. After the reaction mixture is cooled to room temperature, the red crystalline product is collected by suction filtration and washed with cold methanol (3 × 30 mL) to give 0.811 g $XbicH_4$ (71%). ^{1}H NMR: δ 15.37 (d, 1 Hz, 2H, 2-O*H*), 9.39 (d, 1 Hz, 2H, N=C*H*), 7.41 (dd, 8, 1 Hz, 2H, xanthene Ar*H*), 7.19 (t, 8 Hz, 2H, xanthene 2,7-*H*), 7.06 (dd, 8, 1 Hz, 2H, xanthene Ar*H*), 6.81 (s, 2H, catechol Ar*H*), 5.93 (s, 2H, 3-O*H*), 1.72 (s, 6H, C[CH_3]$_2$), 1.44 (s, 18H, ^{t}Bu), 1.40 (s, 18H, ^{t}Bu). $^{13}C\{^1H\}$ NMR ($CDCl_3$): δ 162.98 (N=*C*H), 153.47 (xanthene *C*O), 143.94, 142.55, 140.38, 137.53, 137.53, 131.77, 123.92, 123.88, 118.18, 114.24, 113.90, 35.85 (*C*[CH_3]$_3$), 35.52 (*C*[CH_3]$_3$), 34.82 (*C*[CH_3]$_2$), 33.52 (C[*C*H_3]$_3$), 32.30 (C[*C*H_3]$_2$), 29.51 (C[*C*H_3]$_3$). IR: 3508 (w, ν_{OH}), 3479 (w, ν_{OH}), 3369 (w, ν_{OH}), 2956 (m), 2908 (m), 2871 (m), 1619 (m), 1600 (s), 1558 (m), 1481 (m), 1464 (m), 1437 (s), 1416 (s), 1376 (s), 1364 (s), 1292 (m), 1273 (m), 1247 (s), 1235 (s), 1215 (s), 1204 (s), 1179 (m), 1166 (m), 1157 (m), 1090 (m), 1071 (m), 1039 (w), 1025 (w), 996 (m), 981 (m), 896 (m), 878 (m), 866 (m), 856 (w), 819 (w), 807 (w), 795 (m), 779 (w), 735 (s), 677 (w), 668 (w), 657 (w). UV-vis (CH_2Cl_2): λ_{max} = 296 nm (ε = 31 400 L mol^{-1} cm^{-1}), 343 (32 000 L mol^{-1} cm^{-1}). Anal. calcd for $C_{45}H_{56}N_2O_5$: C, 76.67; H, 8.01; N, 3.97. Found: C, 76.58; H, 7.97; N, 4.36.

[($XbicH_2$)SiPh][HCl_2]. In a 20 mL vial, $XbicH_4$ (102.8 mg, 0.146 mmol) is dissolved in 5 mL of chloroform. Phenyltrichlorosilane (30.7 μL, 0.192 mmol) is added to the solution, which immediately turns dark red. Layering with 10 mL hexanes leads to the deposition of red crystals, which are collected on a glass frit after 3 days, washed with hexanes (3 × 5 mL) and pentane (2 × 5 mL) and dried to yield 91.8 mg [($XbicH_2$)SiPh][HCl_2] (71%). ^{1}H NMR: δ 13.46 (d, 13 Hz, 2H, N*H*), 9.52 (d, 14 Hz, 2H, N=C*H*), 7.73 (d, 8 Hz, 4H, xanthene Ar*H*, *o*-Ph), 7.50 (t, 8 Hz, 2H, xanthene Ar*H*), 7.47 (dd, 8, 2 Hz, 2H, xanthene Ar*H*), 7.28 (m, 3H, *m*-, *p*-Ph), 7.02 (s, 2H, catechol Ar*H*), 1.80 (s, 3H, C[CH_3][CH′$_3$]), 1.68 (s, 3H, C[CH_3][C*H*′$_3$]), 1.59 (s, 18H, ^{t}Bu), 1.50 (s, 18H, ^{t}Bu). $^{13}C\{^1H\}$ NMR: δ 161.44, 159.31, 146.01, 145.37, 143.32, 142.74, 136.27, 134.91, 133.50, 129.99, 128.06, 127.82, 126.78, 126.25, 119.28, 117.70, 108.07, 36.22 (*C*[CH_3]$_3$), 36.00 (*C*[CH_3]$_3$), 34.87 (*C*[CH_3]$_2$), 34.09 (C[*C*H_3]$_3$), 32.65 (C[*C*H_3][CH′$_3$]), 30.60 (C[CH_3][*C*H′$_3$]$_2$), 28.67 (C[*C*H_3]$_3$). $^{29}Si\{^1H\}$ NMR: δ −83.57. IR: 2957 (m), 2913 (m), 2870 (m), 1772 (w), 1734 (w), 1621 (m), 1604 (s), 1592 (s), 1568 (m), 1558 (m), 1478 (s), 1451 (s), 1430 (m), 1401 (w), 1394 (w), 1376 (m), 1361 (m), 1345 (s), 1287 (w), 1256 (m), 1237 (s), 1211 (m), 1195 (m), 1182 (m), 1169 (m), 1119 (m), 1109 (m), 1062 (w), 1036 (m), 1009 (m), 996 (m), 927 (w), 902 (w), 869 (m), 836 (s), 822 (s), 778 (m), 772 (m), 738 (m), 714 (m), 699 (m). UV-vis (CH_2Cl_2) λ_{max} = 365 nm (ε = 27 300 L mol^{-1} cm^{-1}). Anal. calcd for $C_{51}H_{60}Cl_2N_2O_5Si$: C, 69.61; H, 6.87; N, 3.18. Found: C, 68.88; H, 6.45; N, 3.47.

(THF)Li(Xbic)SiPh. A solution of [($XbicH_2$)SiPh][HCl_2] (77.0 mg, 0.088 mmol) in 5 mL of THF is added to excess solid LiO^tBu (28.1 mg, 0.350 mmol) to give a yellow solution. After adding 30 mL benzene, the mixture is filtered to remove LiCl. The solvent is removed *in vacuo* and the residue dissolved in 5 mL THF, layered with 15 mL CH_3CN, and stored in a −37° C freezer. After 4 days, the yellow crystals are filtered and taken out of the glovebox, where the product is washed with 5 mL of water, air-dried for 1 h, then washed with 3 × 5 mL pentane and dried under vacuum overnight to give 65.0 mg (THF)Li(Xbic)SiPh (78%). ^{1}H NMR: δ 9.63 (s, 2H, N=C*H*), 7.60 (d, 8 Hz, 2H, *o*-Ph), 7.41 (dd, 7, 2.5 Hz, 2H, xanthene Ar*H*), 7.30–7.17 (m, 7H), 6.90 (s, 2H, catechol Ar*H*), 3.53 (m, 4H, THF α-*H*), 1.75 (s, 3H, C[CH_3][CH′$_3$]), 1.65 (m, 4H, THF β-*H*), 1.57 (s, 3H, C[CH_3][C*H*′$_3$]), 1.56 (s, 18H, ^{t}Bu), 1.49 (s, 18H, ^{t}Bu). $^{13}C\{^1H\}$ NMR: δ 163.80 (N=C*H*), 150.93, 146.70, 146.03, 141.05, 140.52, 139.44, 136.61, 135.01, 133.16, 129.43, 127.84, 125.19, 123.58, 116.94, 115.21, 114.42, 68.28 (THF α-*C*), 36.26 (*C*[CH_3]$_3$), 35.41 (*C*[CH_3]$_3$), 35.19 (*C*[CH_3][CH′$_3$]), 33.98 (C[*C*H_3]$_3$), 32.02 (C[*C*H_3][CH′$_3$]), 29.50 (C[*C*H_3]$_3$), 29.10 (C[CH_3][*C*H′$_3$]$_2$), 25.99 (THF β-*C*). $^{29}Si\{^1H\}$ NMR: δ −85.12. IR: 3070 (w), 3044 (w), 2984 (w), 2952 (m), 2910 (m), 2866 (m), 1734 (w), 1717 (w), 1699 (w), 1684 (w), 1653 (w), 1613 (w), 1592 (m), 1586 (m), 1568 (w), 1551 (s), 1507 (w), 1465 (m), 1434 (s), 1425 (s), 1401 (m), 1382 (s), 1361 (m), 1340 (w), 1295 (w), 1269 (m), 1237 (s), 1206 (m), 1181 (w), 1170 (w), 1121 (m), 1113 (m), 1100 (s), 1037 (w), 1010 (m), 994 (s), 917 (w), 886 (w), 871 (m), 825 (s), 814 (s), 785 (s), 754 (s), 734 (s), 715 (s), 698 (s). UV-vis (CH_2Cl_2) λ_{max} = 326 nm (ε = 49 100 L mol^{-1} cm^{-1}), 342 (50 000). Anal. calcd for $C_{55}H_{65}LiN_2O_6Si$: C, 74.63; H, 7.40; N, 3.16. Found: C, 75.18; H, 7.23; N, 3.21.

(THF)Na(Xbic)SiPh. The sodium compound is prepared as described for the lithium analogue, using 79.3 mg [($XbicH_2$)SiPh][HCl_2] (0.090 mmol) and 67.1 mg $NaN(SiMe_3)_2$ (0.366 mmol) to yield 41.0 mg (THF)Na(Xbic)SiPh (50%). ^{1}H NMR: δ 9.59 (s, 2H, N=C*H*), 7.61 (d, 7 Hz, 2H, *o*-Ph), 7.46 (dd, 8, 1 Hz, 2H, xanthene Ar*H*), 7.37 (dd, 8, 1 Hz, 2H,

xanthene Ar*H*), 7.29 (t, 8 Hz, 2H, xanthene Ar*H*), 7.20 (m, 3H, *m*- and *p*-Ph), 6.89 (s, 2H, catechol Ar*H*), 3.48 (t, 6.3 Hz, 4H, THF α-*H*), 1.71 (s, 3H, xanthene C[C*H*$_3$][CH′$_3$]), 1.64 (s, 7H, xanthene C[CH$_3$][C*H*′$_3$], THF β-*H*), 1.56 (s, 18H, ^{t}Bu), 1.50 (s, 18H, ^{t}Bu). ^{13}C{^{1}H} NMR: δ 163.48 (N=*C*H), 150.18, 146.75, 145.41, 140.14, 140.13, 139.88, 135.61, 134.34, 132.64, 128.80, 127.44, 124.92, 123.89, 116.96, 114.69, 114.52, 67.90 (THF α-*C*), 35.97 (*C*[CH$_3$]$_3$), 34.96 (*C*[CH$_3$]$_3$), 34.79 (*C*[CH$_3$][CH′$_3$]), 33.59 (C[*C*H$_3$]$_3$), 31.82 (C[*C*H$_3$][CH′$_3$]), 30.50 (C[CH$_3$][*C*H′$_3$]$_2$), 29.16 (C[*C*H$_3$]$_3$), 25.66 (THF β-*C*). ^{29}Si{^{1}H} NMR: δ −86.19. IR: 3067 (w), 2953 (m), 2910 (w), 2868 (w), 1583 (m), 1544 (s), 1465 (m), 1457 (m), 1430 (s), 1399 (m), 1380 (s), 1362 (m), 1339 (m), 1293 (w), 1267 (m), 1233 (s), 1201 (m), 1180 (m), 1169 (w), 1121 (m), 1092 (m), 1036 (w), 1008 (w), 993 (m), 916 (w), 887 (w), 871 (w), 863 (m), 823 (s), 814 (s), 780 (s), 770 (s), 753 (m), 739 (s), 733 (s), 712 (s), 697 (s), 668 (m). UV-vis (CH_2Cl_2) λ_{max} = 314 (ε = 49 000 L mol^{-1} cm^{-1}), 327 (47 600). Anal. calcd for $C_{55}H_{65}N_2NaO_6Si$: C, 73.30; H, 7.27; N, 3.11. Found: C, 73.42; H, 6.93; N, 3.31.

Ag(Xbic)SiPh. A solution of [(XbicH$_2$)SiPh][HCl$_2$] (83.8 mg, 0.095 mmol) in 5 mL of 50 : 50 benzene : THF is added to a 20 mL vial containing silver acetate (63.7 mg, 0.382 mmol). The vial is then capped and taken out of the drybox. The resulting yellow mixture is stirred for 15 min. After filtering through a Celite plug, the solvent is removed *in vacuo*. The yellow solid is collected and washed with 5 mL water and 5 mL acetonitrile. The product is collected and dried under vacuum overnight to yield 46.1 mg Ag(Xbic)SiPh (53%). ^{1}H NMR: δ 9.59 (d, J_{AgH} = 8 Hz, 2H, N=C*H*), 7.63 (d, 7 Hz, 2H, *o*-Ph), 7.45 (d, 7.5 Hz, 2H, xanthene Ar*H*), 7.37 (d, 8 Hz, 2H, xanthene Ar*H*), 7.32 (t, 8 Hz, 2H, xanthene Ar*H*), 7.22 (m, 3H, *m*- and *p*-Ph), 6.86 (s, 2H, catechol Ar*H*), 1.80 (s, 3H, C[C*H*$_3$][CH′$_3$]), 1.52 (s, 18H, ^{t}Bu), 1.50 (s, 3H, C[CH$_3$][C*H*′$_3$]), 1.49 (s, 18H, ^{t}Bu). ^{13}C{^{1}H} NMR: δ 167.07 (N=*C*H), 151.12, 146.96, 146.87, 140.17, 139.81, 139.73, 135.79, 135.59, 135.24, 129.32, 127.76, 125.27, 123.38, 117.44, 114.62, 114.28 (d, J_{AgC} = 2 Hz), 36.47 (*C*[CH$_3$][CH′$_3$]), 36.30 (*C*[CH$_3$]$_3$), 35.26 (*C*[CH$_3$]$_3$), 33.61 (C[*C*H$_3$]$_3$), 30.76 (s, C[*C*H$_3$][CH′$_3$]), 29.45 (C[*C*H$_3$]$_3$), 26.10 (C[CH$_3$][*C*H′$_3$]). ^{29}Si{^{1}H} NMR: δ −88.31. IR: 3070 (w), 3039 (w), 2954 (w), 2907 (w), 2870 (w), 1582 (m), 1568 (w), 1543 (m), 1468 (m), 1430 (s), 1401 (m), 1381 (s), 1360 (m), 1339 (w), 1289 (w), 1266 (m), 1235 (s), 1204 (m), 1182 (m), 1168 (m), 1158 (w), 1120 (m), 1105 (m), 1094 (s), 1031 (w), 1026 (w), 1005 (m), 992 (s), 958 (w), 890 (w), 887 (w), 865 (s), 824 (s), 813 (s), 792 (s), 787 (s), 777 (s), 771 (s), 753 (m), 738 (s), 714 (s), 706 (s), 697 (s), 687 (s), 675 (s), 668 (s). UV-vis (CH_2Cl_2): λ_{max} = 329 nm (ε = 23 600 L mol^{-1} cm^{-1}). Anal. calcd for $C_{51}H_{57}AgN_2O_5Si$: C, 67.02; H, 6.29; N, 3.07. Found: C, 66.11; H, 6.32; N, 3.07.

Electrochemistry

Cyclic voltammograms were performed at a scan rate of 60 mV s^{-1} using a Metrohm Autolab PGSTAT128N potentiostat, with glassy carbon working and counter electrodes and a silver/silver chloride pseudo-reference electrode. The electrodes were connected to the potentiostat through electrical conduits in the drybox wall. Samples were 1 mM in analyte dissolved in CH_2Cl_2, with 0.1 M Bu_4NPF_6 as the electrolyte. Potentials were referenced to ferrocene/ferrocenium at 0 V,[25] with the reference potential established by spiking the test solution with a small amount of ferrocene for XbicH$_4$, [(XbicH$_2$)SiPh][HCl$_2$] and (THF)Li(Xbic)SiPh or decamethylferrocene for (THF)Na(Xbic)SiPh and Ag(Xbic)SiPh (E^o = −0.565 V *vs.* Cp_2Fe^+/Cp_2Fe).[26]

Computational methods

Geometry optimizations were performed on gas-phase [(XbicH$_2$)SiPh]$^+$ and (THF)Li(Xbic)SiPh using density functional theory (B3LYP, 6-31G* basis set), using the Gaussian16 suite of programs.[27] The X-ray structures were used as initial geometries, with all *tert*-butyl and methyl groups replaced by hydrogen. The optimized geometries were confirmed as minima by calculation of vibrational frequencies. Plots of calculated Kohn–Sham orbitals were generated using Gaussview (v. 6.0.16) with an isovalue of 0.03.

X-ray crystallography

Crystals of XbicH$_4$ were grown by slow evaporation from acetone. Crystals of [(XbicH$_2$)SiPh][HCl$_2$]·3CHCl$_3$ were grown by liquid diffusion of hexane into a solution of the complex in chloroform. Crystals of (THF)M(Xbic)SiPh·2THF (M = Li, Na) were grown by diffusion of acetonitrile into a solution of the complex in tetrahydrofuran. Crystals of Ag(Xbic)SiPh·3CD$_2$Cl$_2$ deposited from the reaction mixture of [(XbicH$_2$)SiPh][HCl$_2$] and Ag_2O in CD_2Cl_2. Crystals were placed in inert oil before being transferred to the cold N_2 stream of either a Bruker Apex II or a Bruker Kappa X8-Apex-II CCD diffractometer. The data were reduced, correcting for absorption, using the program SADABS. The structures were all solved using direct methods. All nonhydrogen atoms were refined anisotropically. Hydrogen atoms were found on difference maps and refined isotropically, except for lattice solvents and as noted, where they were placed in calculated positions with their thermal parameters tied to the isotropic thermal parameters of the atoms they are bonded (1.5× for methyl, 1.2× for all others): in [(XbicH$_2$)SiPh][HCl$_2$]·3CHCl$_3$, all hydrogens except for those bonded to nitrogen or chlorine; in (THF)Li[(Xbic)SiPh], hydrogens on the bound THF; in Ag(Xbic)SiPh·3CD$_2$Cl$_2$, all hydrogens on methyl groups.

In [(XbicH$_2$)SiPh][HCl$_2$]·3CHCl$_3$, four chloroforms in the asymmetric unit were found and refined, but there was additional diffuse electron density in the unit cell that was treated using the program SQUEEZE.[28] The total amount of electron density found in the void spaces was 256 electrons per unit cell, corresponding to approximately 4 $CHCl_3$ molecules, for a total of 12 in the unit cell (3 per formula unit). Disorder was noted in one of the HCl_2 anions in this structure, as well as in C63 of the THF bound to Li in (THF)Li(Xbic)SiPh·2THF, and one of the lattice dichloromethanes in Ag(Xbic)SiPh·3CD$_2$Cl$_2$. In each case the disorder was modeled by refining the disordered atom in two sites with a total occupancy of unity, fixing the thermal parameters of the two sites to be equal and allowing their relative occupancies to refine.

Table 1 Crystal data

	$XbicH_4$	$[(XbicH_2)SiPh][HCl_2]\cdot 3CHCl_3$	(THF)Li(Xbic)SiPh·2THF	(THF)Na(Xbic)SiPh·2THF	$Ag(Xbic)SiPh\cdot 3CD_2Cl_2$
Molecular formula	$C_{45}H_{56}N_2O_5$	$C_{54}H_{63}Cl_{11}N_2O_5Si$	$C_{63}H_{81}LiN_2O_8Si$	$C_{63}H_{81}N_2NaO_8Si$	$C_{54}H_{57}AgCl_6D_6N_2O_5Si$
Formula weight	704.91	1238.10	1029.32	1045.37	1174.76
T/K	120(2)	120(2)	120(2)	120(2)	120(2)
Crystal system	Triclinic	Triclinic	Monoclinic	Monoclinic	Monoclinic
Space group	$P\bar{1}$	$P\bar{1}$	$P2_1/c$	$P2_1/c$	$P2_1/c$
λ/Å	0.71073 (Mo Kα)	0.71073 (Mo Kα)	0.71073 (Mo Kα)	0.71073 (Mo Kα)	0.71073 (Mo Kα)
Total data collected	49 269	123 098	124 873	129 520	154 871
No. of indep reflns	10 186	30 965	14 612	14 183	14 700
R_{int}	0.0539	0.0216	0.0452	0.0712	0.0275
Obsd refls [$I > 2\sigma(I)$]	6747	24 316	10 816	10 326	13 067
a/Å	9.8219(5)	16.3173(8)	16.0349(9)	16.104(2)	15.9942(18)
b/Å	14.8289(8)	17.8374(8)	19.6695(12)	19.806(3)	19.485(2)
c/Å	15.3393(8)	21.3223(11)	17.5883(11)	17.777(2)	17.562(2)
α/°	68.6189(17)	89.6599(17)	90	90	90
β/°	80.0462(18)	81.8825(7)	93.404(2)	94.0682(2)	92.0777(16)
γ/°	73.9409(17)	84.0998(16)	90	90	90
V/Å^3	1992.71(18)	6111.1(5)	5537.5(6)	5656.0(13)	5469.6(11)
Z	2	4	4	4	4
μ/mm^{-1}	0.076	0.565	0.100	0.106	0.731
Crystal size/mm	0.25 × 0.20 × 0.11	0.69 × 0.50 × 0.40	0.34 × 0.28 × 0.25	0.24 × 0.20 × 0.20	0.31 × 0.26 × 0.21
No. refined params	693	1287	908	936	691
R_1, wR_2 [$I > 2\sigma(I)$]	0.0503, 0.1164	0.0538, 0.1347	0.0617, 0.1625	0.0588, 0.1440	0.0603, 0.1702
R_1, wR_2 [all data]	0.0896, 0.1349	0.0706, 0.1459	0.0887, 0.1826	0.0876, 0.1616	0.0674, 0.1773
Goodness of fit	1.025	1.020	1.021	1.042	1.116

Calculations used SHELXTL (Bruker AXS),[29] with scattering factors and anomalous dispersion terms taken from literature.[30] Further details are in Table 1.

Results and discussion

Ligand design and synthesis

4,5-Diamino-9,9-dimethylxanthene has been used as a rigid scaffold to position a pair of organic[31] or inorganic[32–34] complexes in proximity to one another. Molecular models suggested that the bis(catecholimine) of this structure would be well organized to allow binding of a metal center to an "upper pocket" consisting of the two catecholates, with the catecholates forming a roughly square O_4 array. A "lower pocket" consisting of the two imine nitrogens, the xanthene oxygen, and the two catecholate oxygens *ortho* to the imines, could potentially accommodate a second metal center with a pentagonal arrangement of ligands, similar to that afforded by 15-crown-5.

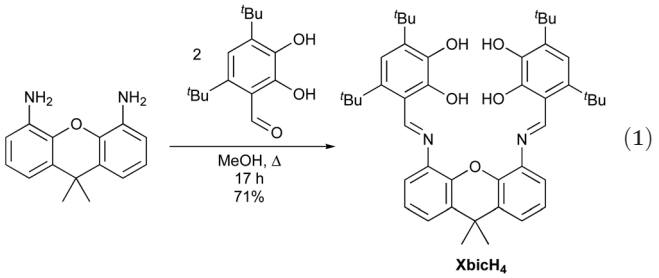

(1)

The bis(catecholimine) $XbicH_4$ is prepared in one step in moderate yield (eqn (1)) by the Schiff base condensation of 4,5-diamino-9,9-dimethylxanthene[24,35–37] and 4,6-di-*tert*-butyl-2,3-dihydroxybenzaldehyde[18,19] in refluxing methanol. The reaction requires overnight reflux to ensure complete conversion to the bis(imine); the somewhat more forcing conditions compared to other imines[20] may be due to the presence of an *ortho* substituent in the diaminoxanthene.

The ^{1}H and ^{13}C NMR spectra of $XbicH_4$ are consistent with a C_{2v}-symmetric product, with the two geminal methyl groups equivalent to each other. The two O*H* resonances are very separated, with the 3-OH group resonating at δ 5.93 ppm in CD_2Cl_2 and the 2-OH group far downfield at δ 15.37. The downfield chemical shift is characteristic of a strong intramolecular hydrogen bond, but is not useful in distinguishing between the imine-phenol and the enamino-ketone tautomers. More diagnostic are the ^{13}C shift of the aromatic carbon bonded to oxygen (150–155 ppm for the imino-phenol,[38] ~180 ppm for the enaminoketone[39]) and the *HC*=N*H* coupling constant (~0 for the iminophenol, 5–12 Hz for the enaminoketone[40]). The upfield ^{13}C shift (δ 153.5 in $CDCl_3$) and small $^3J_{HH}$ (1.0 Hz in CD_2Cl_2, undetectable in $CDCl_3$) in $XbicH_4$ indicate that the compound exists largely or exclusively as the imino-phenol tautomer in solution. This is consistent with past observations that this tautomer is strongly favored for catecholaldimines without *tert*-butyl substituents.[41]

The imino-phenol tautomer is also observed in the solid state (Fig. 1), with the OH hydrogens found on difference Fourier maps and refined successfully. One of the catechol rings is roughly in the same plane as the xanthene ring (angle between planes = 26.9°), while the other catechol ring is turned 63.7° from this plane, resulting in the two catchol rings being essentially perpendicular to each other. The 2-OH groups are strongly hydrogen bonded to the imine nitrogens

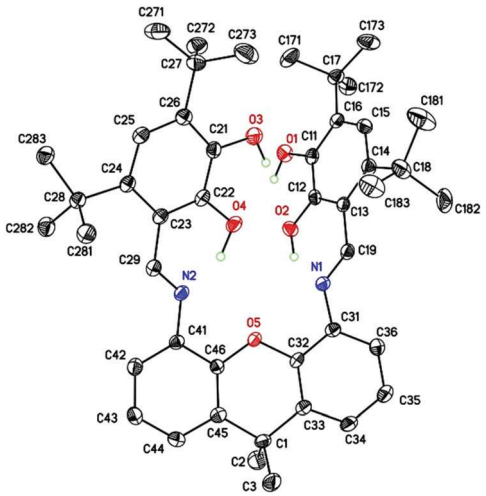

Fig. 1 Thermal ellipsoid plot of $XbicH_4$. Hydrogen atoms bonded to carbon have been omitted for clarity.

(H2–N1 = 1.66 Å, H4–N2 = 1.58 Å), with the 3-OH groups forming longer hydrogen bonds to the *ortho* oxygens (H1–O2 = 2.07 Å, H3–O4 = 2.03 Å), but there are no intermolecular hydrogen bonds in the crystal. This contrasts with catecholaldimines lacking the 4-*tert*-butyl group, where the 3-OH group participates in intermolecular hydrogen bonding in the solid state.[41,42]

Metalation of $XbicH_4$ to form a square pyramidal cationic silicon complex

$XbicH_4$ reacts with phenyltrichlorosilane in chloroform under inert atmosphere to give a dark red bis(catecholate-iminium) complex $[(XbicH_2)SiPh][HCl_2]$ (eqn (2)), which can be purified by crystallization from chloroform/hexanes and isolated in good yield. The compound is stable under inert atmosphere, but hydrolyzes within a few hours on exposure to air, regenerating $XbicH_4$.

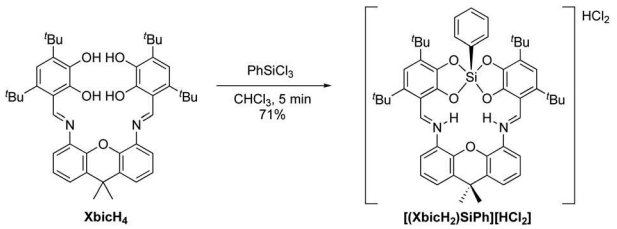

(2)

NMR spectra of $[(XbicH_2)SiPh][HCl_2]$ indicate that the compound is C_s-symmetric, with the inequivalence of the geminal methyl groups indicating that the two faces of the Xbic ligand are inequivalent. The large coupling constant (13 Hz) between the downfield signal at 13.46 ppm and the imine C*H* proton at 9.52 ppm clearly indicates that the hydrogen has shifted from the phenolic oxygen to the imine nitrogen, with the chemical shift confirming that it retains a strong intramolecular hydrogen bond. This iminium-catecholate motif is well known in metal complexes of catecholimines,[20,21,43,44] and allows these ligands to act as overall uninegative versions of catecholates. The ^{29}Si resonance at δ −83.57 falls in the narrow range observed for anionic five-coordinate organosilicon bis(catecholate) anions.[45]

Consistent with the solution NMR data, the $[(XbicH_2)SiPh]^+$ cation has an iminium-catecholate structure in the solid state, with the hydrogens clearly observable on the nitrogen atoms (Fig. 2). There is relatively little contribution of the enaminoketone resonance structure, as judged, for example, by the very similar C11–O1 and C12–O2 distances (1.350(5) Å and 1.335(9) Å, respectively) (Table 2). Metrical oxidation state cal-

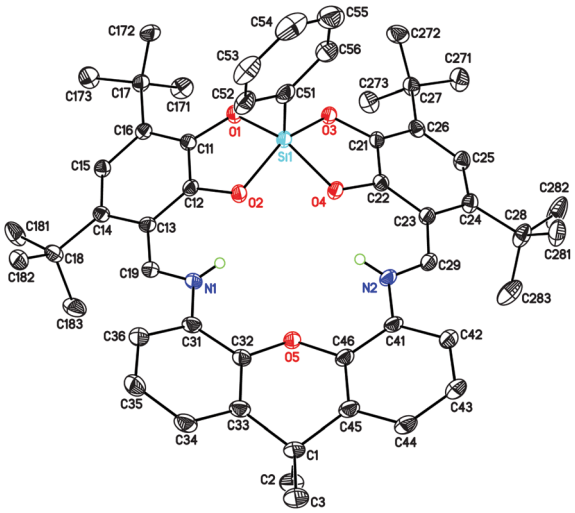

Fig. 2 Thermal ellipsoid plot of the cation of $[(XbicH_2)SiPh][HCl_2]\cdot 3CHCl_3$. Hydrogen atoms bonded to carbon have been omitted for clarity, and only one of the two crystallographically inequivalent cations is shown.

Table 2 Selected metrical data for $[(XbicH_2)SiPh][HCl_2]\cdot 3CHCl_3$ [a]

Bond distances/Å	
Si–O1	1.717(17)
Si–O2	1.78(3)
Si–C5	1.849(2)
C11–O1	1.350(5)
C12–O2	1.335(9)
τ[52]	0.16(5)
Metrical oxidation state (MOS)[46]	−2.07(19)
Bond angles/°	
O1–Si–O2	87.4(4)
O1–Si–O3	87.54(12)
O2–Si–O4	82.0(3)
O1–Si–C5	108(2)
O2–Si–C5	103(3)
O1–Si–O4 (β)	154(2)
O2–Si–O3 (α)	144(2)

[a] Where applicable, chemically equivalent parameters in the crystal structure have been averaged between the two crystallographically independent complexes in the unit cell and between values related by the (noncrystallographic) mirror planes through the center of the molecules. The cited esd's combine the variance of the independent values with the esd's of each individual observation.

culations for the dioxolene rings[46] confirm that they are well described as fully reduced catecholates. The strong hydrogen bonds between the iminiums and O2/O4 of the catecholates (hydrogen bond distance of 1.85(11) Å) elongate these silicon–oxygen bonds by about 0.07 Å compared to the bonds to the other oxygens of the catecholates.

The silicon complex is cationic, with a bichloride (HCl_2^-) counterion. The identity of the counterion is established by the observation of paired chlorine atoms with close Cl–Cl contacts of 3.118(5) Å, similar to literature values of 3.14–3.22 Å.[47] The [Cl–*H*–Cl] hydrogens were found on difference Fourier maps and are unsymmetrically disposed, as seen in other salts.[47] The bichloride proton was not observed in the ^{1}H NMR.

Organosilicon bis(catecholates) are universally found to be five-coordinate, unless the organic group has a donor atom capable of chelating to silicon.[48–51] The solid state structure confirms this for [(XbicH$_2$)SiPh][HCl$_2$], showing a square pyramidal geometry (τ = 0.12, with τ = 0 corresponding to an ideal square pyramid and τ = 1 to an ideal trigonal bipyramid[52]) with an apical phenyl group. Organosilicon bis(catecholates) do not have a strong intrinsic preference for either limiting five-coordinate geometry,[53] so it is unclear what role the Xbic ligand plays in determining the geometry at silicon. Hydrogen bonding to catecholate has been suggested to contribute to a tendency towards a square pyramidal structure,[54,55] but the effect is not strong,[56] with many examples of trigonal bipyramidal RSi(Cat)$_2$ structures with hydrogen bonding[53,57] and square pyramidal ones without hydrogen bonding.[58,59] In any case, it is clear that the Xbic ligand is capable of accommodating a metal in a square array of oxygen donors.

Complexation of univalent cations in the lower pocket

Clean removal of both iminium hydrogens in [(XbicH$_2$)SiPh][HCl$_2$] can be achieved using lithium *tert*-butoxide or sodium hexamethyldisilazide in tetrahydrofuran, forming light yellow (THF)Li(Xbic)SiPh or light orange (THF)Na(Xbic)SiPh, respectively (eqn (3)). The reactions are fast, with color changes seen within seconds of adding the base. The products are stable to air and moisture in the solid state (they can be washed with water to remove any coprecipitated alkali metal halide).

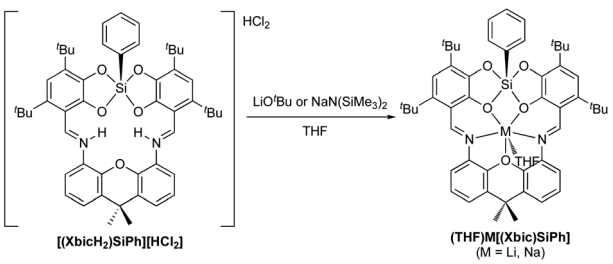

(3)

NMR spectroscopy confirms that both iminium hydrogens have been removed, with the peak downfield of 10 ppm in [(XbicH$_2$)SiPh]$^+$ disappearing and the corresponding N=C*H* resonance being observed as a singlet. Crystallography shows that the alkali metal binds in the lower pocket of the complexes, which are isostructural (Fig. 3 and Fig. S1†). Both alkali

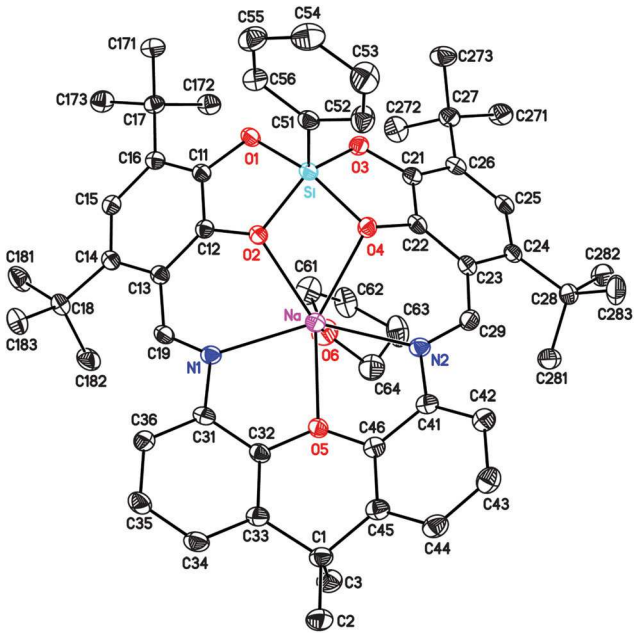

Fig. 3 Thermal ellipsoid plot of (THF)Na(Xbic)SiPh·2THF. Hydrogen atoms and lattice solvent molecules are omitted for clarity.

metals adopt a six-coordinate, pentagonal monopyramid geometry, with five binding atoms being supplied by the lower pocket of the Xbic ligand and the sixth by a tetrahydrofuran molecule coordinated to the face opposite the phenyl group on silicon. While the pentagonal monopyramid is a much less common coordination geometry than the octahedron, it has been previously observed in lithium[60–62] and sodium[63–65] complexes of 15-crown-5, to which the N_2O_3 lower pocket of Xbic bears a strong resemblance.

Replacing two protons with an alkali metal in the lower pocket causes several changes in the geometry at silicon. The alkali metals appear to be weaker Lewis acids than the protons, as the Si–O2 distances decrease by about 0.02 Å in the alkali metal complexes. The geometry at silicon is still best described as square pyramidal, but is more distorted toward trigonal bipyramidal (τ = 0.38 [M = Li] or 0.36 [M = Na]).

The protons in the lower pocket of [(XbicH$_2$)SiPh][HCl$_2$] can also be replaced with silver by treatment with a variety of silver reagents, forming air- and moisture-stable Ag(Xbic)SiPh (eqn (4)). Reaction is slower than with alkali metal bases, with

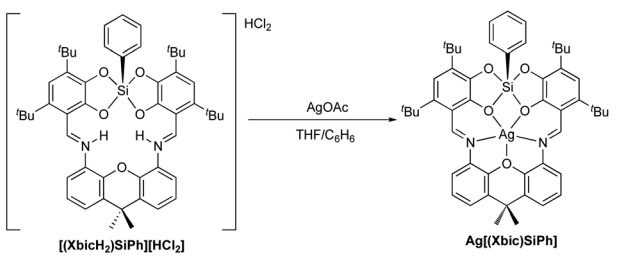

(4)

reaction times in benzene ranging from 20 min (AgOAc or AgOTf) to one week (Ag$_2$O). Differences in rate are probably

due largely to differences in solubility of the silver compounds; reactions are faster in THF/benzene mixtures than in neat benzene. The ^{1}H NMR of Ag(Xbic)SiPh is consistent with C_s symmetry for the complex, and shows $^{3}J_{AgH}$ = 8 Hz to the imine C*H* at 9.59 ppm in CD_2Cl_2.

In the solid state, silver binds in the lower pocket of the ligand, with a roughly pentagonal geometry (Fig. 4). The Ag–O5 distance is long (2.606(2) Å, Table 3), which is typical of bond distances to the aryl ethers observed in complexes of silver bound to benzo-15-crown-5 derivatives (2.60(11) Å avg.).[66–69] The silver ion lies 0.90 Å out of the N_2O_3 plane, displaced in the direction of the Si–Ph bond. In the solid state, a sixth coordination site (apical in the pentagonal pyramid) is occupied by coordination to an arene (the C34–C35 bond in the xanthene unit of an inversion-related molecule). The silver is nearly equidistant to the pair of xanthene carbons (2.547(3) Å and 2.596(3) Å), which is uncommon, with most silver–arene bonds being asymmetric, with short bonds of 2.45–2.49 Å and long bonds of 2.6–2.9 Å.[70,71] This axial bond is either lost in solution or is very labile, judging from the C_s symmetry displayed in the NMR spectra of Ag(Xbic)SiPh.

The pentacoordinate silicon in Ag(Xbic)SiPh adopts a distorted square pyramidal structure, with the τ value of 0.37

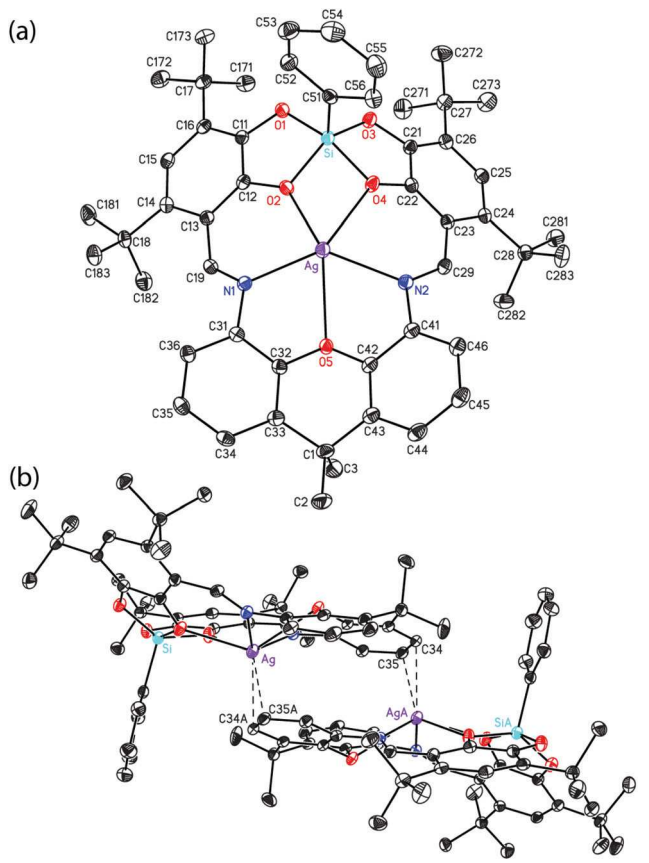

Fig. 4 Thermal ellipsoid plots of Ag(Xbic)SiPh·3CD_2Cl_2. Hydrogen atoms and lattice solvent molecules are omitted for clarity. (a) Monomer. (b) Inversion-related pair of molecules, highlighting intermolecular η^2-arene coordination.

Table 3 Selected metrical data for (THF)M(Xbic)SiPh·2THF (M = Li, Na) and M(Xbic)SiPh·3CD_2Cl_2 (M = Ag)

	M = Li	M = Na	M = Ag
Bond distances/Å			
Si–O1	1.7346(15)	1.7488(15)	1.739(2)
Si–O2	1.7483(14)	1.7487(15)	1.754(2)
Si–O3	1.7111(14)	1.7164(14)	1.719(2)
Si–O4	1.7786(15)	1.7910(15)	1.786(2)
Si–C51	1.860(2)	1.866(2)	1.872(3)
M–O2	2.074(4)	2.2437(16)	2.402(2)
M–O4	2.158(4)	2.3140(16)	2.473(2)
M–O5	2.408(4)	2.3539(16)	2.606(2)
M–N1	2.280(4)	2.3522(18)	2.379(3)
M–N2	2.300(4)	2.3511(19)	2.394(3)
M–O6	2.016(4)	2.3167(18)	
Ag–C34A			2.547(3)
Ag–C35A			2.596(3)
MOS (ring 1)	−2.10(15)	−2.09(19)	−2.04(19)
MOS (ring 2)	−2.07(14)	−2.03(15)	−2.03(19)
τ	0.380(2)	0.361(2)	0.370(3)
Bond angles/°			
O1–Si–O4 (β)	158.94(7)	159.06(7)	159.64(12)
O2–Si–O3 (α)	136.12(7)	137.42(7)	137.48(12)
O2–M–N1	77.00(13)	74.96(6)	73.36(8)
O2–M–O4	65.75(11)	61.93(5)	56.73(7)
N1–M–O5	69.96(11)	71.61(6)	66.18(8)
N2–M–O4	74.39(12)	74.14(6)	70.65(8)
N2–M–O5	68.90(11)	70.57(6)	64.93(8)

essentially identical to that shown by the alkali metal complexes. The apical arene ligand in the silver complex is *syn* to the Si–Ph group, whereas the coordinated THF ligand is *anti* to the Si–Ph group in the alkali metal complexes. Apparently, the geometry around silicon becomes appreciably more trigonal bipyramidal when the Xbic ligand is fully deprotonated, but is relatively insensitive to the size or nature of the metal that coordinates in the pocket.

Reactivity and bonding of (Xbic)Si complexes

The five-coordinate silicon atom in $[(XbicH_2)SiPh]^+$ does not appear to be significantly Lewis acidic, with no binding being observed upon addition of alcohols such as methanol or nitrogen donors such as pyridine or triethylamine. The nitrogen bases remove one of the iminium hydrogens to give neutral (XbicH)SiPh, though we were unable to isolate this compound in pure form.

Density functional theory (DFT) calculations on $[(XbicH_2)SiPh]^+$ show that the two highest-energy occupied molecular orbitals are based on the two combinations of the high-lying redox-active orbitals[72] of the catecholate groups (Fig. 5). The in-phase combination is stabilized relative to the out-of-phase combination by 0.30 eV, possibly because it donates into the Si–Ph σ* orbital (Fig. 5a). A similar orbital stabilization of 0.29 eV is calculated in (THF)Li(Xbic)SiPh. This $\pi \rightarrow \sigma^*$ donation may explain in part the low Lewis acidity of the five-coordinate silicon in these complexes.

Cyclic voltammograms of the (Xbic)Si complexes in dichloromethane show only irreversible redox events (Fig. S17–

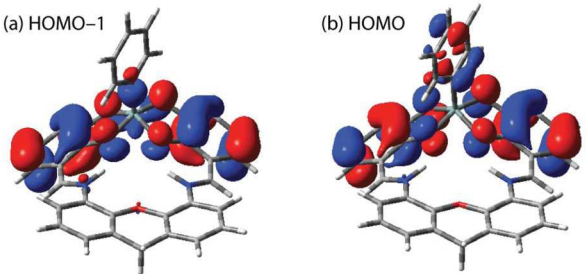

Fig. 5 High-lying occupied orbitals in $[(XbicH_2)SiPh]^+$. (a) HOMO–1 (b) HOMO.

S21†), with the peak anodic current of the first oxidation of $[(XbicH_2)SiPh][HCl_2]$ occurring at 0.81 V *vs.* Cp_2Fe^+/Cp_2Fe in CH_2Cl_2. Replacing the two protons in the lower pocket with a univalent ion results in a decrease in the peak potential. The ease of oxidation increases with the increasing ionic radius of the metal in the lower pocket (and correspondingly longer metal-catecholate oxygen distances), with $E_{p,a}$ in M(Xbic)SiPh decreasing from 0.68 V to 0.42 V to 0.16 V for M = Li, Na and Ag, respectively. For comparison, $[K(18\text{-c-}6)][RSi(O_2C_6H_4)_2]$ salts show irreversible oxidations at 0.16–0.45 V *vs.* Cp_2Fe^+/Cp_2Fe (in DMF).[73]

Attempts to react the complexes with inner-sphere oxidants have been unsuccessful. $[(XbicH_2)SiPh][HCl_2]$ does not react with diisopropyl azodicarboxylate, and shows only slight decomposition over the course of a week with iodobenzene dichloride. (THF)Li(Xbic)SiPh does not react with Selectfluor over the course of several days at room temperature.

Conclusions

A new catecholimine ligand, $XbicH_4$, based on 4,5-diaminoxanthene, contains an upper O_4 pocket consisting of a square bis(catecholate) fragment and a lower N_2O_3 pocket formed from the two imines, two of the catecholate oxygens, and the xanthene oxygen atom. Reaction with phenyltrichlorosilane affords $[(XbicH_2)SiPh][HCl_2]$, with silicon bound in the upper pocket. In this complex, silicon adopts a nearly ideal square pyramidal geometry, which is distorted somewhat towards a trigonal bipyramidal geometry on replacement of the two protons in the lower pocket with univalent cations lithium, sodium, or silver. These univalent cations adopt pentagonal monopyramidal geometries in the solid state with the alkali metals binding an apical THF and silver binding an arene bond from a xanthene group of a neighboring molecule. The compounds undergo only irreversible electrochemistry and do not bind Lewis bases at the five-coordinate silicon.

Conflicts of interest

There are no conflicts to declare.

Acknowledgements

This work was supported by the US National Science Foundation (Grant CHE-1465104). We thank Dr Allen G. Oliver for assistance with X-ray crystallography.

Notes and references

1 C. G. Pierpont, *Coord. Chem. Rev.*, 2001, **216–217**, 99–125.
2 C. G. Pierpont and H. H. Downs, *Inorg. Chem.*, 1977, **16**, 2970–2972.
3 S. Roy, B. Sarkar, D. Bubrin, M. Niemeyer, S. Zális, G. K. Lahiri and W. Kaim, *J. Am. Chem. Soc.*, 2008, **130**, 15230–15231.
4 T. Marshall-Roth, S. C. Liebscher, K. Rickert, N. J. Seewald, A. G. Oliver and S. N. Brown, *Chem. Commun.*, 2012, **48**, 7826–7828.
5 A. H. Randolph, N. J. Seewald, K. Rickert and S. N. Brown, *Inorg. Chem.*, 2013, **52**, 12587–12598.
6 P. Chaudhuri, M. Hess, J. Müller, K. Hildenbrand, E. Bill, T. Weyhermüller and K. Wieghardt, *J. Am. Chem. Soc.*, 1999, **121**, 9599–9610.
7 P. N. O'Shaughnessy, P. D. Knight, C. Morton, K. M. Gillespie and P. Scott, *Chem. Commun.*, 2003, 1770–1771.
8 K. S. Min, T. Weyhermüller, E. Bothe and K. Wieghardt, *Inorg. Chem.*, 2004, **43**, 2922–2931.
9 R. Metzinger, S. Demeshko and C. Limberg, *Chem. – Eur. J.*, 2014, **20**, 4721–4735.
10 M. K. Mondal, A. Tiwari and C. Mukherjee, *Chem. Commun.*, 2016, **52**, 11995–11998.
11 D. D. Swanson, K. M. Conner and S. N. Brown, *Dalton Trans.*, 2017, **46**, 9049–9057.
12 T. Marshall-Roth and S. N. Brown, *Dalton Trans.*, 2015, **44**, 677–685.
13 K. J. Blackmore, N. Lai, J. W. Ziller and A. F. Heyduk, *J. Am. Chem. Soc.*, 2008, **130**, 2728–2729.
14 C. Mukherjee, T. Weyhermüller, E. Bothe and P. Chaudhuri, *Inorg. Chem.*, 2008, **47**, 11620–11632.
15 A. I. Nguyen, R. A. Zarkesh, D. C. Lacy, M. K. Thorson and A. F. Heyduk, *Chem. Sci.*, 2011, **2**, 166–169.
16 L. D. Loomis and K. N. Raymond, *Inorg. Chem.*, 1991, **30**, 906–911.
17 A. du Moulinet d'Hardemare, S. Torelli, G. Serratrice and J.-L. Pierre, *BioMetals*, 2006, **19**, 349–366.
18 M. Arsenyev, E. Baranov, S. Chesnokov and G. Abakumov, *Acta Crystallogr., Sect. E: Struct. Rep. Online*, 2013, **69**, o1565.
19 M. V. Arsenyev, E. V. Baranov, A. Y. Fedorov, S. A. Chesnokov and G. A. Abakumov, *Mendeleev Commun.*, 2015, **25**, 312–314.
20 M. V. Arsenyev, E. V. Baranov, S. A. Chesnokov, V. K. Cherkasov and G. A. Abakumov, *Russ. Chem. Bull., Int. Ed.*, 2013, **62**, 2394–2400.
21 S. V. Baryshnikova, E. V. Bellan, A. I. Poddel'sky, M. V. Arsenyev, I. V. Smolyaninov, G. K. Fukin,

A. V. Piskunov, N. T. Berberova, V. K. Cherkasov and G. A. Abakumov, *Eur. J. Inorg. Chem.*, 2016, **2016**, 5230–5241.
22 A. I. Poddel'sky, M. V. Arsen'ev, L. S. Okhlopkova, I. V. Smolyaninov and G. K. Fukin, *Russ. J. Coord. Chem.*, 2017, **43**, 843–851.
23 M. V. Arsen'ev, L. S. Okhlopkova, A. I. Poddel'skii and G. K. Fukin, *Russ. J. Coord. Chem.*, 2018, **44**, 162–168.
24 S. A. Nagamani, Y. Norikane and N. Tamaoki, *J. Org. Chem.*, 2005, **70**, 9304–9313.
25 N. G. Connelly and W. E. Geiger, *Chem. Rev.*, 1996, **96**, 877–910.
26 D. Lionetti, A. J. Medvecz, V. Ugrinova, M. Quiroz-Guzman, B. C. Noll and S. N. Brown, *Inorg. Chem.*, 2010, **49**, 4687–4697.
27 M. J. Frisch, G. W. Trucks, H. B. Schlegel, G. E. Scuseria, M. A. Robb, J. R. Cheeseman, G. Scalmani, V. Barone, G. A. Petersson, H. Nakatsuji, X. Li, M. Caricato, H. P. Hratchian, J. V. Ortiz, A. F. Izmaylov, J. L. Sonnenberg, D. Williams-Young, F. Ding, F. Lipparini, F. Egidi, J. Goings, B. Peng, A. Petrone, T. Henderson, D. Ranasinghe, V. G. Zakrzewski, J. Gao, N. Rega, G. Zheng, W. Liang, M. Hada, M. Ehara, K. Toyota, R. Fukuda, J. Hasegawa, M. Ishida, T. Nakajima, Y. Honda, O. Kitao, H. Nakai, T. Vreven, K. Throssell, J. A. Montgomery Jr., J. E. Peralta, F. Ogliaro, M. J. Bearpark, J. J. Heyd, E. N. Brothers, K. N. Kudin, V. N. Staroverov, T. A. Keith, R. Kobayashi, J. Normand, K. Raghavachari, A. P. Rendell, J. C. Burant, S. S. Iyengar, J. Tomasi, M. Cossi, J. M. Millam, M. Klene, C. Adamo, R. Cammi, J. W. Ochterski, R. L. Martin, K. Morokuma, O. Farkas, J. B. Foresman and D. J. Fox, *Gaussian 16, Revision B.01*, Gaussian, Inc., Wallingford CT, 2016.
28 P. van der Sluis and A. L. Spek, *Acta Crystallogr., Sect. A: Found. Crystallogr.*, 1990, **46**, 194–201.
29 G. M. Sheldrick, *Acta Crystallogr., Sect. A: Found. Crystallogr.*, 2008, **64**, 112–122.
30 *International Tables for Crystallography*, ed. A. J. C. Wilson, Kluwer Academic Publishers, Dordrecht, The Netherlands, 1992, vol. C.
31 B. C. Hamann, N. R. Branda and J. Rebek, *Tetrahedron Lett.*, 1993, **34**, 6837–6840.
32 A. Panunzi, F. Giordano, I. Orabona and F. Ruffo, *Inorg. Chim. Acta*, 2005, **358**, 1217–1224.
33 A. Bheemaraju, J. W. Beattie, Y. Danylyuk, J. Rochford and S. Groysman, *Eur. J. Inorg. Chem.*, 2014, 5865–5873.
34 T. S. Hollingsworth, R. L. Hollingsworth, T. Rosen and S. Groysman, *RSC Adv.*, 2017, **7**, 41819–41829.
35 G. Malaisé, L. Barloy and J. A. Osborn, *Tetrahedron Lett.*, 2001, **43**, 7417–7419.
36 K.-J. Chang, Y.-J. An, H. Uh and K.-S. Jeong, *J. Org. Chem.*, 2004, **69**, 6556–6563.
37 A. E. Metz, K. Ramalingam and M. C. Kozlowski, *Tetrahedron Lett.*, 2015, **56**, 5180–5184.
38 R. Dobosz, A. Skotnicka, Z. Rozwadowski, T. Dziembowska and R. Gawinecki, *J. Mol. Struct.*, 2010, **979**, 194–199.
39 T. Dziembowska, Z. Rozwadowski, A. Filarowski and P. E. Hansen, *Magn. Reson. Chem.*, 2001, **39**, S67–S80.
40 R. Gawinecki, A. Kuczek, E. Kolehmainen, B. Ośmiałowski, T. M. Krygowski and R. Kauppinen, *J. Org. Chem.*, 2007, **72**, 5598–5607.
41 H. Pizzala, M. Carles, W. E. E. Stone and A. Thevand, *J. Chem. Soc., Perkin Trans. 2*, 2000, 935–939.
42 H. Pizzala, M. Carles, W. E. E. Stone and A. Thevand, *J. Mol. Struct.*, 2000, **526**, 261–268.
43 M. Albrecht, S. Burk, R. Stoffel, A. Lüchow, R. Fröhlich, M. Kogej and C. A. Schalley, *Eur. J. Inorg. Chem.*, 2007, 1361–1372.
44 H. A. Rudbari, M. Khorshidifard, B. Askari, N. Habibi and G. Bruno, *Polyhedron*, 2015, **100**, 180–191.
45 J. A. Cella, J. D. Cargioli and E. A. Williams, *J. Organomet. Chem.*, 1980, **186**, 13–17.
46 S. N. Brown, *Inorg. Chem.*, 2012, **51**, 1251–1260.
47 J. Emsley, *Chem. Soc. Rev.*, 1980, **9**, 91–124.
48 F. Carré, G. Cerveau, C. Chuit, R. J. P. Corriu and C. Réyé, *Angew. Chem., Int. Ed. Engl.*, 1989, **28**, 489–491.
49 F. Carré, C. Chuit, R. J. P. Corriu, A. Mehdi and C. Reyé, *J. Organomet. Chem.*, 1993, **446**, C6–C8.
50 F. Carré, C. Chuit, R. J. P. Corriu, A. Fanta, A. Mehdi and C. Reyé, *Organometallics*, 1995, **14**, 194–198.
51 A. A. Korlyukov, A. G. Shipov, E. P. Kramarova, V. V. Negrebetskii and Y. I. Baukov, *Russ. Chem. Bull., Int. Ed.*, 2008, **57**, 2093–2100.
52 A. W. Addison, T. N. Rao, J. Reedijk, J. van Rijn and G. C. Verschoor, *J. Chem. Soc., Dalton Trans.*, 1984, 1349–1356.
53 R. Tacke, M. Pülm, I. Richter, B. Wagner and R. Willeke, *Z. Anorg. Allg. Chem.*, 1999, **625**, 2169–2177.
54 R. R. Holmes, R. O. Day, V. Chandrasekhar and J. M. Holmes, *Inorg. Chem.*, 1985, **24**, 2009–2015.
55 J. Sperlich, J. Becht, M. Mühleisen, S. A. Wagner, G. Mattern and R. Tacke, *Z. Naturforsch.*, 1993, **48b**, 1693–1706.
56 R. R. Holmes, R. O. Day, J. J. Harland and J. M. Holmes, *Organometallics*, 1984, **3**, 347–353.
57 R. Tacke, A. Lopez-Mras, J. Sperlich, C. Strohmann, W. F. Kuhs, G. Mattern and A. Sebald, *Chem. Ber.*, 1993, **126**, 851–861.
58 R. R. Holmes, R. O. Day, J. J. Harland, A. C. Sau and J. M. Holmes, *Organometallics*, 1984, **3**, 341–347.
59 R. R. Holmes, R. Day, V. Chandrasekhar, J. J. Harland and J. M. Holmes, *Inorg. Chem.*, 1985, **24**, 2016–2020.
60 U. Olsher, R. M. Izatt, J. S. Bradshaw and N. K. Dalley, *Chem. Rev.*, 1991, **91**, 137–164.
61 R. Boulatov, B. Du, E. A. Meyers and S. G. Shore, *Inorg. Chem.*, 1999, **38**, 4554–4558.
62 S. Chadwick, U. Englich and K. Ruhlandt-Senge, *Organometallics*, 1997, **16**, 5792–5803.
63 B. Schreiner, K. Dehnicke and D. Fenske, *Z. Anorg. Allg. Chem.*, 1993, **619**, 1127–1131.
64 D. B. Dell'Amico, F. Calderazzo, N. Pasqualetti, R. Hübener, C. Maichle-Mössmer and J. Strähle, *J. Chem. Soc., Dalton Trans.*, 1995, 3917–3924.

65 H. Nöth and M. Warchhold, *Eur. J. Inorg. Chem.*, 2004, 1115–1124.
66 M. Wen, M. Maekawa, M. Munakata, Y. Suenaga and T. Kuroda-Sowa, *Inorg. Chim. Acta*, 2002, **338**, 111–118.
67 Y. V. Fedorov, O. A. Federova, E. N. Andryukhina, S. P. Gromov, M. V. Alfimov, L. G. Kuzmina, A. V. Churakov, J. A. K. Howard and J.-J. Aaron, *New J. Chem.*, 2003, **27**, 280–288.
68 A. I. Vedernikov, L. G. Kuz'mina, Y. A. Strelenko, J. A. K. Howard and S. P. Gromov, *Russ. Chem. Bull., Int. Ed.*, 2010, **59**, 927–940.
69 M. Barboiu, A. Meffre, Y.-M. Legrand, E. Petita, L. Marin, M. Pinteala and A. V. D. Lee, *Supramol. Chem.*, 2014, **26**, 223–228.
70 K. Shelly, D. C. Finster, Y. J. Lee, W. R. Scheidt and C. A. Reed, *J. Am. Chem. Soc.*, 1985, **107**, 5955–5959.
71 E. A. H. Griffith and E. L. Amma, *J. Am. Chem. Soc.*, 1974, **96**, 743–749.
72 A. N. Erickson and S. N. Brown, *Dalton Trans.*, 2018, **47**, 15583–15595.
73 V. Corce, L.-M. Chamoreau, E. Derat, J.-P. Goddard, C. Ollivier and L. Fensterbank, *Angew. Chem., Int. Ed.*, 2015, **54**, 11414–11418.